Strain-Dependent Differences in Oxygen-Induced Retinopathy in the Inbred Rat

Peter van Wijngaarden,[1] *Douglas J. Coster,*[1] *Helen M. Brereton,*[1] *Ian L. Gibbins,*[2] *and Keryn A. Williams*[1]

Purpose. To examine the susceptibilities of different rat strains to oxygen-induced retinopathy, a model of human retinopathy of prematurity.

Methods. Litters of newborn rats of five inbred strains (Fischer 344 [F344], Dark Agouti [DA], Sprague-Dawley [SD], Wistar-Furth [WF], Lewis [LEW]) and one outbred strain (Hooded Wistar [HW]) were maintained in room air or were exposed to alternating 24-hour cycles of hyperoxia (80% oxygen in air) and normoxia (21% oxygen in air) for 14 days and were killed for analysis, either immediately (postnatal day 14, [P14]) or after 4 days in room air (P18). The fluorophore-conjugated isolectin GS-IB4 was used to label the endothelial cells of wholemounted retinas, and digital images were analyzed for avascular area and for morphologic abnormalities.

Results. Exposure to cyclic hyperoxia inhibited retinal vascularization in all strains relative to age-matched room air control animals. Total retinal avascular area at P14 after cyclic hyperoxia varied significantly among strains ($P < 0.001$). Avascular areas were smallest for the albino F344, WF, and LEW strains; larger for the albino SD strain; and largest for the pigmented DA and HW strains. Susceptibility to hyperoxic vascular attenuation was associated with ocular pigmentation, but neither with body mass nor with natural variation in litter size. Room air exposure for 4 days after cyclic hyperoxia was also associated with strain-related differences in retinal vascularization and with abnormalities in vascular morphology ($P < 0.05$). For all strains, the size of the avascular retinal area at P14 was predictive of the severity of morphologic abnormality at P18.

Conclusions. Marked and consistent variations in the response of different inbred rat strains to cyclic hyperoxia were observed, suggestive of a genetic component to oxygen-induced retinopathy. (*Invest Ophthalmol Vis Sci.* 2005;46:1445–1452) DOI:10.1167/iovs.04-0708

The neovascular retinopathies, characterized by the proliferation of aberrant retinal vessels, are a major cause of visual disability worldwide.[1–3] Disease processes as varied as retinopathy of prematurity (ROP), diabetes, sickle cell anemia, and retinal vein occlusion all converge on a common pathologic pathway characterized by retinal hypoperfusion, leading to hypoxia and neovascularization.[4,5]

From the Departments of [1]Ophthalmology and [2]Anatomy and Histology, Flinders University of South Australia, Adelaide, Australia.

Supported by the National Health and Medical Research Council of Australia, the Ophthalmic Research Institute of Australia, the Diabetes Australia Research Trust, and the Flinders Medical Centre Research Foundation, Australia.

Submitted for publication June 15, 2004; revised November 11 and December 22, 2004; accepted January 2, 2005.

Disclosure: **P. van Wijngaarden**, None; **D.J. Coster**, None; **H.M. Brereton**, None; **I.L. Gibbins**, None; **K.A. Williams**, None

The publication costs of this article were defrayed in part by page charge payment. This article must therefore be marked "advertisement" in accordance with 18 U.S.C. §1734 solely to indicate this fact.

Corresponding author: Keryn A. Williams, Department of Ophthalmology, Flinders Medical Centre, Bedford Park 5042 SA, Australia; keryn.williams@flinders.edu.au.

Animal models of oxygen-induced retinopathy have provided pivotal insights into the pathogenesis of this shared pathway. Rodent retinal vascularization, in contrast to that of humans, occurs primarily ex utero.[6,7] This process is driven by regional tissue hypoxia (*physiological hypoxia*), which accompanies retinal growth and maturation.[8] As retinal oxygen demand exceeds its supply by diffusion from the choroidal circulation, retinal sentinel cells (principally Müller cells) release a range of hypoxia-inducible angiogenic factors. Vascular endothelial growth factor (VEGF) has been well established as a central proangiogenic factor in this process.[9–12] Expression of a suite of angiogenic factors, including VEGF, is primarily mediated by the heterodimeric transcription factor, hypoxia-inducible factor (HIF)-1, which accumulates in hypoxia.[13–15] In this manner, retinal vascularization is closely matched to the oxygen requirement.

Exposure of neonatal rats to high levels of inspired oxygen (hyperoxia) is thought to increase the diffusion of oxygen from the choroidal circulation, such that retinal physiological hypoxia is abrogated.[9,16,17] This has the consequence of allowing retinal development to continue in the presence of an attenuated circulation. When hyperoxic exposure is terminated, the mature, sparsely vascularized retina becomes acutely hypoxic and the resultant surge in angiogenic factors leads to aberrant retinal vascularization that resembles the pathologic features of human proliferative retinopathies.[18,19] Accordingly, animal models of oxygen-induced retinopathy are central to studies of the human disease and its treatment.

At present, few factors beyond birth-weight and gestational age are useful in stratifying neonates for risk of ROP. Insights gained from animal models may be of value to this end. In the oxygen-exposed rodent, the extent of the avascular area in the peripheral retina is highly correlated with both the risk of neovascularization and the severity of the neovascular response.[11,18,20] In other studies the severity of retinopathy has been associated with metabolic acidosis,[21] increased inspired carbon dioxide levels,[22–24] growth retardation,[25,26] early postnatal insulin-like growth factor-1 deficiency,[27,28] and with elevations in nitric oxide[29] and adenosine levels.[30] Retinopathy has also been linked with cyclooxygenase-2[31] and tyrosine kinase c-*abl* expression.[32] Furthermore, an association has been identified between ocular pigmentation and susceptibility to hypoxia-induced angiogenesis in the rat.[33] Other studies have demonstrated a greater susceptibility of albino rats than of pigmented rats to ischemic retinal injury[34] and to retinal gliosis after trauma and inflammation.[35] We sought to examine further the effects of strain and pigmentation on susceptibility to oxygen-induced retinopathy in the rat, with the purpose of enhancing understanding of the model and providing insights into human ROP susceptibility.

Methods

Experimental Animals

Five inbred rat strains (Fischer 344 [F344], Dark Agouti [DA], Sprague-Dawley [SD], Wistar-Furth [WF], Lewis [LEW]), each derived from more than 20 consecutive brother–sister matings, and one outbred

TABLE 1. Rat Strains, Genetic Inbreeding Status, Pigmentation and Source

Strain	Inbred	Pigmentation	Eye Color	Mean Litter Size	Source
Fischer 344 (F344)	Yes	Albino	Red	11	Flinders University, Adelaide, SA, Australia
Wistar-Furth (WF)	Yes	Albino	Red	6	Flinders University, Adelaide, SA, Australia
Lewis (LEW)	Yes	Albino	Red	8	Animal Resources Centre, Perth, WA, Australia
Sprague-Dawley (SD)	Yes	Albino	Red	6	Flinders University, Adelaide, SA, Australia
Dark Agouti (DA)	Yes	Pigmented (agouti)	Dark brown	8	Institute of Medical and Veterinary Science, Adelaide, SA, Australia
Hooded Wistar (HW)	No	Pigmented (black)	Dark brown	8	Flinders University, Adelaide, SA, Australia

strain (Hooded Wistar [HW]) were used (Table 1). Lineage records and allozyme electrophoresis confirmed genetic integrity. Four albino and two pigmented strains were selected to examine the effects of ocular pigmentation on oxygen-induced retinopathy. Pigmentation and eye color are listed in Table 1. Rats were allowed unlimited access to water and rat chow and were exposed to a 12-hour light–dark cycle. Room temperature was maintained at 24°C. Ambient humidity was maintained at between 40% and 55% for all experimental groups. Animals were killed with an inhaled overdose of halothane anesthesia. All animal experiments were approved by the institutional Animal Welfare Committee and conformed to the ARVO Statement for the Use of Animals in Ophthalmic and Vision Research.

Exposure of Neonatal Rats to Cyclic Oxygen Levels

Female rats and their newborn litters were housed in a custom-built, humidified chamber (Fig. 1). The cyclic oxygen exposure protocol was a modification of those used in other studies of rat oxygen-induced retinopathy.[18,20,36–38] Litters were placed in the chamber within 12 hours of birth and exposed to alternating 24-hour cycles of hyperoxia (80% O_2) and normoxia (21% O_2) for the first 14 days of life (cyclic oxygen). An anesthetic blender (Bennett AO-1; CIG Medishield-Ramsay, Melbourne, Victoria, Australia) and high-flow oxygen regulator (Anaequip; Adelaide, South Australia, Australia) were used to deliver oxygen to the chamber at 25 L/min. Oxygen levels within the chamber were continuously monitored with a fuel-cell oxygen monitor (Oxygen Monitor, model 5550; Hudson, Temecula, CA) and were recorded with a data logger (Tinytalk II; Gemini Dataloggers, Ltd., Chichester, UK) for subsequent analysis (Gemini Logger Manager, ver. 2.6; Gemini Dataloggers Ltd.). An oxygen concentration of 80% ± 1% was maintained for the duration of hyperoxic cycles. Survival rates were in excess of 95% for hyperoxia-exposed neonatal rats, and there was no obvious maternal oxygen toxicity. Rats reared in room air were used as control subjects. Pups from at least two different litters of each of the six rat strains studied were analyzed at each exposure endpoint to distinguish interstrain from intrastrain variation. In those instances in which an entire litter was not used for analysis, pups were selected at random. Mean litter sizes of each strain are provided in Table 1.

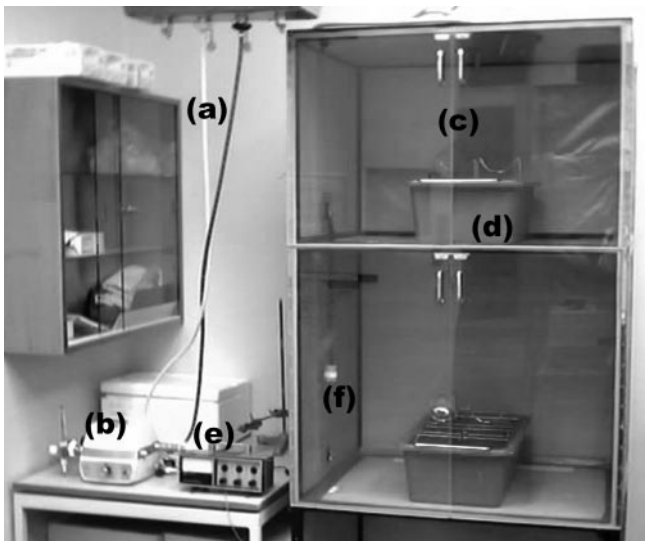

FIGURE 1. Oxygen-exposure chamber. Air and oxygen (a) were mixed with an anesthetic blender (b) and delivered to the chamber (c) with a high-flow regulator. The chamber was constructed from a wooden cabinet, which was mounted with Perspex doors and made airtight. Four rat cages (d) could be housed simultaneously. Oxygen levels within the chamber were continuously monitored with a fuel cell oxygen sensor (f) and an oxygen monitor (e) attached to a data recorder. Humidity was maintained at 50%.

Tissue Processing and Isolectin Histochemistry

After the 14-day period of cyclic hyperoxia, rats were removed to room air and killed for analysis immediately (postnatal day [P]14), to assess oxygen-induced vascular attenuation, or 4 days later (P18), to evaluate the extent of hypoxia-induced vasoproliferation. Control rats raised in room air were killed at P14 for comparison with rats exposed to cyclic oxygen. Enucleated eyes were fixed in 2% wt/vol paraformaldehyde in 1 M phosphate buffered saline (PBS; pH 7.4) at 4°C for 90 minutes and dissected according to the method of Chan-Ling.[39] Four equally spaced radially oriented incisions were used to flatten each retina. Retinal wholemounts were transferred, inner aspect up, to chrome-alum–coated glass slides, and the endothelial cells stained with fluorophore-conjugated *Griffonia simplicifolia* isolectin GS-IB4[40] (Alexa Fluor 488 conjugate; Molecular Probes, Eugene, OR) according to a modification of the method of Cunningham et al.[41] In brief, retinas were permeabilized with prechilled 70% (vol/vol) ethanol for 30 minutes at 4°C, followed by PBS-1% (vol/vol) Triton X-100 (Ajax Chemicals, Sydney, Australia) for 20 minutes. Each retina was washed twice with PBS and incubated with 50 μL of 4 μg/mL isolectin in PBS overnight. Retinas were washed in PBS seven times, covered with PBS and glycerol (2:1 vol/vol; pH 7.4) and coverslipped. In all cases, retinal dissection and histochemistry were performed within 6 hours of enucleation.

Image Analysis of Labeled Retinas

The right retina of each animal was used for image analysis. Imaging was performed within 12 hours of lectin labeling with a fluorescence microscope (BX50F; Olympus Optical Co., Ltd., Tokyo, Japan) equipped with a charge-coupled device (CCD)-digital camera (Photometrics Coolsnap *fx*; Roper Scientific, Trenton, NJ) and image acquisition software (RS Image, ver 1.01; Roper Scientific). Sequential, overlapping high-resolution images of the entire retina were captured with a 4× objective. Images were manually arranged, merged to construct a montage image of the retina (Photoshop, ver. 7.0; Adobe Systems Inc., San Jose, CA) and analyzed using image-analysis software (ImageJ, ver. 1.30; available by ftp at zippy.nimh.nih.gov/ or at http://rsb.info.nih.gov/nih-image; developed by Wayne Rasband, National Institutes of Health, Bethesda, MD). Each montage was analyzed in a window measuring 20 × 20 cm on a high-definition LCD computer monitor (17-in. Apple Studio Display; Apple Computer, Cupertino, CA). Avascular areas were manually outlined and measured as a percentage of the total retinal area by a masked observer. Repeat analyses by the same observer were highly concordant (mean difference 2.1% ±

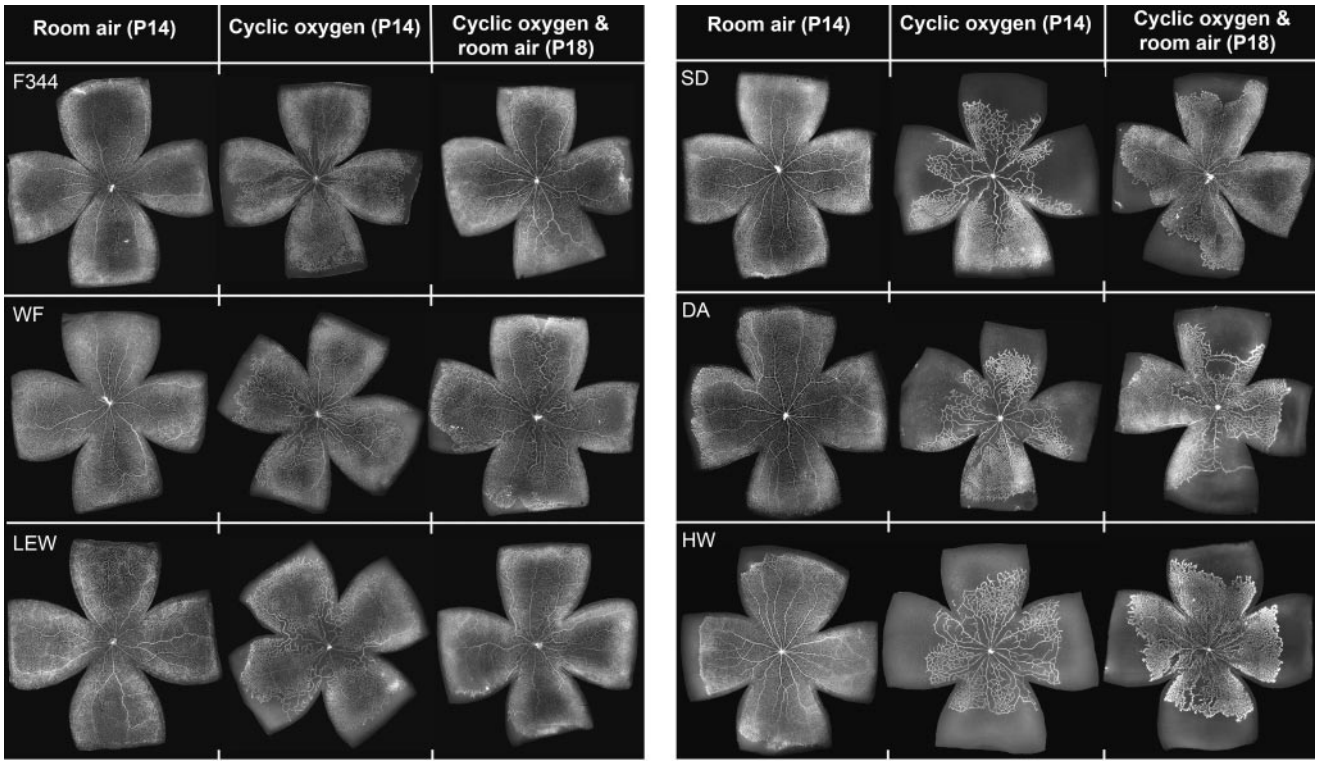

FIGURE 2. Comparison of retinal vascular area and morphology by strain, for room air and hyperoxia-exposed rats. Digital montages of retinal wholemounts labeled with fluorophore-conjugated isolectin GS-IB4. Representative retinas of rats reared in room air and cyclic hyperoxia (80%) are provided for each strain. Strain-dependent differences in vascular attenuation followed 14 days of oxygen exposure (P14). Differences in vascular morphology and proliferation were apparent after a 4-day period of relative hypoxia in room air (P18).

1.9%). The central avascular zone was defined as the capillary-free region surrounding the optic nerve head. Peripheral avascular zones were capillary-free regions not in continuity with the optic nerve head.

A semiquantitative system was used to grade vascular morphology. The retinal montages of P18 cyclic oxygen-exposed rats were compared with reference images of room air-exposed controls. Montages were scored for vascular morphologic abnormalities and tortuosity. Morphologic abnormalities were defined as features not seen in the course of normal retinal vascularization, including regions of exceptionally dense vascular budding, vascular ridges, marked vascular dilatation, and neovascular tufts. Neovascular tufts were defined as vascular projections anterior to the superficial vascular plexus. Each retinal quadrant was divided into thirds to give a total of 12 clock hours of retina, and each clock hour was scored for the presence (1) or absence (0) of any of these morphologic abnormalities.[20,38,42] The tortuosity of retinal vessels was assessed by eye in masked fashion, using reference images for comparison. First-order vessels were considered along their entire length, and an overall grading was determined for each retina as normal (1), minimally increased (2), moderately increased (3), or markedly increased (4).

Statistical Analyses

Before statistical analysis, percentages were transformed with the angular (arcsin) transformation to normalize the variances of the data.[43] The transformed data were analyzed by analysis of variance, including repeated-measures designs when appropriate. Comparisons between subsets of data were made with preplanned, single degree-of-freedom contrasts, Ryan-Einot-Gabriel-Welsch F tests (REGWF tests) or Bonferroni tests, with significance levels (α) set at 0.05 in each case. Summary data are expressed as the mean with 95% confidence interval (95% CI). χ^2 and Kruskal Wallis tests were used for the analysis of vascular morphology data. All statistical analysis was performed using SPSS software (SPSS, ver. 11.0.2; SPSS Inc., Chicago, IL).

RESULTS

Strain-Related Retinal Responses to Room Air Exposure

Control rats raised in room air for 1 day segregated into two groups with respect to retinal avascular area ($F_{(5,15)} = 13.7$, $P < 0.001$): avascular areas were slightly but significantly larger for the F344, WF, and DA strains (mean, 86.5%; 95% CI, 85.6%–87.4%), than for the SD, LEW, and HW strains (mean, 81.2%; 95% CI, 80.2%–82.3%). Significant differences were also found in total avascular retinal area among control rats of different strains at P14 ($F_{(5,60)} = 33.4$; $P < 0.001$; Figs. 2, 3). The central retina was fully vascularized in all strains by P14, and the differences were due entirely to variation in peripheral retinal vascularization. The peripheral avascular areas of the HW and DA strains were larger than those of other strains ($P < 0.05$). Although the avascular area of HW rats was more than twice that of F344 rats, it was still <10% of the total retinal area (Table 2, Fig. 3).

Strain-Related Retinal Responses to Cyclic Oxygen Exposure

Rats exposed to cyclic oxygen for 14 days had significantly larger areas of avascular retina (overall mean, 41.6%; 95% CI, 39.6%–48.6%) than rats exposed to room air for the same period (overall mean, 4.9%; 95% CI, 4.5%–5.2%; $F_{(11,30)} = 1760.4$; $P < 0.001$; Figs. 2, 3). The effect of oxygen exposure on total retinal avascular area differed among strains ($F_{(5,70)} = 73.2$; $P < 0.001$). Avascular areas were smallest in the F344, WF, and LEW strains, larger in the SD strain, and largest in the DA and HW strains ($P < 0.05$ per comparison).

At P14, all strains exposed to cyclic hyperoxia exhibited avascular areas in the central retina that were not seen in rats

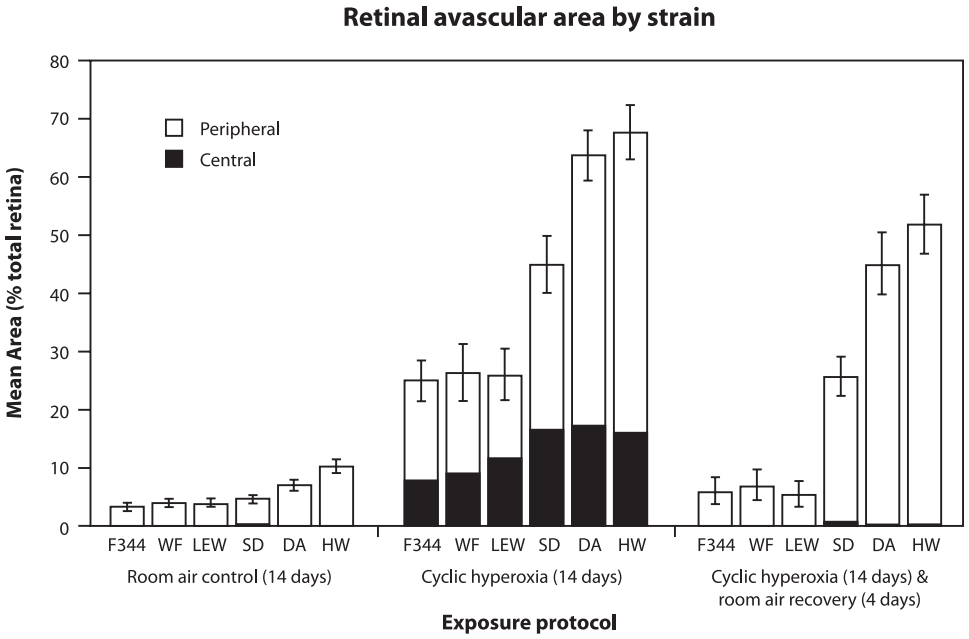

FIGURE 3. Newborn rats of six strains were exposed to room air or cyclic hyperoxia for 14 days before analysis of retinal avascular area (P14). A third group was exposed to cyclic hyperoxia for 14 days followed by room air for 4 days (P18). Mean central avascular area (peripapillary capillary-free zone) and peripheral avascular area (peripheral capillary-free zone, not in continuity with the optic nerve head) are presented as a percentage of the total retinal area. Error bars are 95% CIs for total avascular area.

exposed to room air. The extent of central avascular area differed among strains ($F_{(5,70)} = 38.4$; $P < 0.001$). Those of the F344, WF, and LEW were smaller than those of other strains ($P < 0.05$).

Rats exposed to cyclic oxygen had larger avascular areas in the peripheral retina at P14 (mean, 28%; 95% CI, 26.8%–29.3%) than did those exposed to room air (mean, 4.8%; 95% CI, 4.2%–5.5%; $F_{(11,30)} = 1096.6$; $P < 0.001$). The size of peripheral avascular areas differed among strains ($F_{(5,70)} = 72.5$; $P < 0.001$). Peripheral avascular areas of DA and HW rats were more than double those of F344, WF, and LEW rats ($P < 0.05$). The peripheral avascular area of SD rats was less than those of DA and HW rats but greater than those of other strains ($P < 0.05$ per comparison). Mean litter sizes for oxygen-exposed rats ranged from 6 to 10 for all strains, and no association was found between litter size and retinal avascular area at P14 (linear regression, $r = 0.17$; $P = 0.13$).

At P18 (14 days of cyclic oxygen followed by 4 days in room air) rats had total retinal avascular areas that were intermediate in size between those of the control and the oxygen-exposed groups at P14 ($P < 0.05$ per comparison; Table 2; Figs. 2, 3). Comparison between oxygen-exposed rats at the P14 and P18 time-points yielded two key findings: (1) in all strains central retinal vascularization was nearly complete by P18 and (2) F344, WF, and LEW rats had smaller peripheral avascular areas at P18 than at P14 ($P < 0.05$ per comparison). In contrast, there were no significant changes in peripheral avascular area in SD, DA, and HW rats between these two time-points ($P > 0.05$).

Vascular Morphology

Assessment of the retinal vascular morphology of rats at P18 is presented in Table 3. Figures 2 and 4 provide representative images. There were significant differences in clock hours of vascular morphologic abnormality among strains ($\chi^2_{(60)} = 142.7$; $P < 0.001$). The F344, WF, and LEW strains had fewer clock hours of abnormality than did the SD strain which, in turn, had fewer than the DA and HW strains. Tortuosity of the major retinal vessels was minimally increased for F344, DA, and HW rats, moderately increased for WF rats and markedly increased for LEW and SD rats, relative to room air control subjects.

Body Mass

There were significant strain differences in body mass among control rats raised in room air for 14 days ($F_{(5,60)} = 23.5$; $P < 0.001$; Table 4). SD rats were significantly heavier than HW

TABLE 2. Retinal Avascular Areas of Rats by Strain, after Room Air Exposure or Cyclic Hyperoxia

	Day 1 (Control)		Day 14 (Control)		Day 14 (Oxygen)		Day 18* (Oxygen and Room Air Recovery)	
Strain	***n*†**	**% Avascular‡**	***n*†**	**% Avascular‡**	***n*†**	**% Avascular‡**	***n*†**	**% Avascular‡**
F344	4	85.5 (84.0–87.0)	12	2.9 (2.3–3.5)	18	24.6 (21.2–28.2)	11	5.4 (3.3–8.0)
WF	3	87.2 (85.5–88.9)	9	3.5 (2.8–4.3)	9	26.0 (21.1–31.2)	10	6.5 (4.1–9.4)
LEW	3	81.1 (79.0–83.0)	10	3.4 (2.8–4.2)	11	25.6 (21.3–30.3)	10	4.9 (2.8–7.4)
SD	4	81.0 (79.2–82.7)	14	4.3 (3.7–5.1)	12	44.8 (39.8–49.7)	18	25.4 (22.0–28.9)
DA	4	86.9 (85.5–88.3)	11	6.6 (5.7–7.6)	14	63.6 (59.1–67.9)	10	44.8 (39.5–50.2)
HW	3	81.8 (79.8–83.7)	10	9.9 (8.7–11.1)	12	67.7 (63.0–72.2)	11	51.7 (46.6–56.8)
TOTAL	21	84.1 (83.3–84.7)	66	4.8 (4.5–5.2)	76	41.6 (39.6–43.6)	70	20.7 (18.4–21.6)

* Exposed to cyclic hyperoxia for 14 days followed by 4 days of sustained room air exposure.
† Number of animals.
‡ Mean avascular area as a percentage of total retinal area (95% CI).

TABLE 3. Abnormal Retinal Vascular Morphology and Vascular Tortuosity of Cyclic Oxygen-Exposed Rats Analyzed by Strain at P18

Strain	*n**	Abnormal Morphology† Median (Range)	Vascular Tortuosity‡ Median (Range)
F344	11	2 (2–4)	2 (1–2)
WF	10	3 (0–7)	3 (2–4)
LEW	10	3 (0–5)	4 (3–4)
SD	18	7 (2–9)	4 (3–4)
DA	10	11 (8–12)	2 (2–3)
HW	11	12 (9–12)	2 (2–3)

* Number of rats.

† Clock hours (0–12) of retina with morphological abnormality, including vascular budding, vascular ridges, vascular dilatation, and neovascular tufts.

‡ Vascular tortuosity (1–4) from normal (1), to markedly increased (4).

rats, which in turn were heavier than rats of other strains ($P < 0.05$ per comparison). Across all strains oxygen exposure had a small, but statistically significant inhibitory effect on mass (mean difference, 1.67 g; 95% CI, 0.36–2.98 g; $P = 0.013$). However, when mass was used as a covariate, there was no change in the strength of association between strain and retinal avascular area. Only 10% of the strain difference in avascular area was attributable to differences in mass ($r^2 = 0.10$).

DISCUSSION

This study has identified marked and consistent variation in the response of different inbred rat strains to cyclic hyperoxia in a model of oxygen-induced retinopathy. Significant inhibition of retinal vascularization occurred in newborn rats of all strains after exposure to 14 days of cyclic hyperoxia. However the extent of this inhibition differed significantly among strains and was associated with ocular pigmentation, but not with body mass. Those rats that were exposed to the relative hypoxia of room air for 4 days, after 14 days of cyclic oxygen, underwent complete central vascularization. Peripheral vascularization was incomplete, however, and differed significantly in extent among strains, as did vascular morphologic abnormalities.

Two distinct patterns of retinal vascularization were observed. Those strains that were relatively resistant to cyclic oxygen exposure—the F344, WF, and LEW—had comparatively small avascular areas in the peripheral retina at P14. During the 4-day after exposure period, these strains underwent complete central vascularization, with near complete vascularization of the retinal periphery. Vascular architecture was relatively normal, and few morphologic abnormalities were identified. In contrast, those strains that were more susceptible to cyclic oxygen exposure—the SD, DA, and HW—had large peripheral avascular territories at P14. During the period of relative hypoxia, there was dense and disordered vasoproliferation both centrally and in those peripheral regions that were already vascularized at P14. The retinal vascular morphology in these strains (SD, HW, and DA) was highly abnormal, with dense tufts of endothelial cells, distended central vessels, and grossly dilated vascular buds at the avascular periphery.

In studies of the effects of different hyperoxic exposures on retinal vascularization in the SD rat, a strong association has been identified between the extent of retinal avascular area at the cessation of hyperoxia and the development of neovascularization after subsequent room air exposure.[11,18,20] The present study confirms these findings and demonstrates that the susceptibility to hyperoxic vascular attenuation and subsequent vascular abnormality differs significantly among strains. Of note, vascular tortuosity, a marker of disease severity in human ROP ("plus" disease) bore no obvious relationship to either the degree of retinal vascularization or to other morphologic abnormalities.[44]

In contrast to the F344, WF, and LEW strains, no significant vascularization of the avascular retinal periphery was observed during the period of relative hypoxia (P14–P18) for those strains most susceptible to hyperoxic vascular attenuation (SD, DA, and HW). However, when these rats were examined at later time points, they all exhibited complete retinal vascularization (data not presented). The basis for this delay in peripheral vascularization remains in question. It may be that the large avascular areas in the retinas of these strains are subjected to a more profound hypoxic insult after room air exposure than those of more vascularized strains. The delay in vascularization may therefore relate to transient ischemic compromise of glial cells that ordinarily play critical roles in vascular patterning of the retina, or to disruption of other mediators of vascular development, such as extracellular matrix proteases and cellular adhesion molecules.[9,45–47]

In all strains, central retinal vascularization occurred at a more rapid rate than peripheral vascularization during the period of relative hypoxia. The central retina was vascularized in all strains at birth, and exposure to hyperoxia was associated with vasoconstriction of the central vessels[18,48] and later with endothelial cell death.[49] Revascularization of the central retina is likely to have been facilitated by surviving endothelial cells, and residual extracellular matrix may have aided the ingrowth of nascent vessels. Furthermore angioblasts, important in developmental retinal vascularization, would be expected to have more ready access to the central retina than to more peripheral regions.[50,51]

A small but significant strain difference was found in the extent of retinal vascularization among control rats exposed to room air for 14 days. Control rats of those strains relatively resistant to cyclic hyperoxia, the F344, WF, and LEW, had smaller avascular areas than those of strains susceptible to hyperoxia, the HW and DA. Although a marginally slower rate of retinal vascularization in room air conditions may predispose to increased susceptibility to hyperoxia, it is unlikely to constitute the sole basis for the observed differences in susceptibility. Other strain-dependent genetic factors are likely to be involved. Differences in the regulatory effects of oxygen tension on retinal angiogenesis, such as the ubiquitination and degradation of the constitutively expressed α subunit of HIF-1, or in glial cell sensitivity to hyperoxia, may be responsible.[14] Nunes et al.[32] have implicated the nonreceptor tyrosine kinase c-*abl* in oxygen-induced changes in retinal VEGF mRNA expression in the mouse. Alterations in the expression of c-*abl* or other mediators of oxygen-regulated gene expression may be responsible for the strain differences observed in the present study.

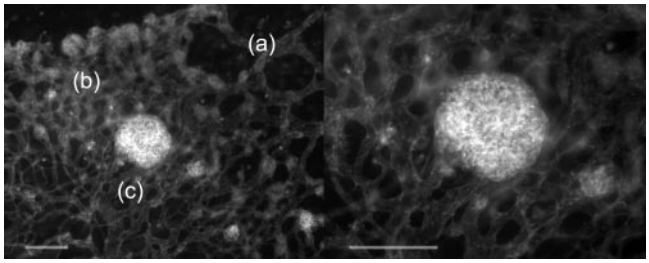

FIGURE 4. A representative image of vascular morphologic abnormalities in the retina of an 18-day-old SD rat exposed to cyclic hyperoxia for the first 14 days of life. Dilated vessels (a) and dense capillary networks (b) are apparent. A large glomerular neovascular tuft (c) is seen projecting anterior to the underlying retina and is shown at higher magnification in the right-hand panel. Scale bar, 100 μm.

TABLE 4. Relationship between Rat Body Mass and Exposure to Room Air or Cyclic Oxygen

Strain	Day 14 (Control)		Day 14 (Oxygen)		Day 18 (Oxygen and Room Air Recovery)	
	*n**	Body Mass Mean g (95% CI)	*n**	Body Mass Mean g (95% CI)	*n**	Body Mass Mean g (95% CI)
F344	12	24.4 (22.1–26.6)	18	21.2 (19.4–23.0)	11	26.7 (24.4–29.0)
WF	9	26.3 (23.8–28.9)	9	25.3 (22.8–27.9)	10	28.8 (26.3–31.2)
LEW	10	27.1 (24.7–29.5)	11	26.9 (24.6–29.2)	10	36.7 (34.3–39.1)
SD	14	37.5 (35.5–39.6)	12	36.6 (34.4–38.8)	18	45.9 (44.1–47.8)
DA	11	24.0 (21.7–26.3)	14	22.5 (20.5–24.6)	10	31.9 (29.5–34.3)
HW	10	33.2 (30.7–35.6)	12	29.9 (27.7–32.1)	11	41.2 (38.8–43.5)

* Number of animals.

Other strain-dependent differences in angiogenesis in the rat are known. Pandey et al.[52] have identified a quantitative trait locus (Edpm5) that contributes to the marked differences in susceptibility of F344 and Brown Norway (BN) rats to angiogenesis in a model of estrogen-induced prolactinoma. In another model, Wang et al. [53] reported that the impaired angiogenesis of spontaneous hypertensive rats, relative to SD rats, is associated with reduced expression of both the VEGF receptor KDR and membrane type 1 matrix metalloproteinase. Angiogenesis has also been shown to vary within rat strains. Kitzmann et al.[54] suggested that significant differences in the severity of oxygen-induced retinopathy between two different groups of inbred SD rats point to a genetic basis for angiogenic susceptibility. Further investigation of these and other postulated risk factors[27,29–31] may identify the basis for the heterogeneity identified in this work.

A previous study of the pigmented BN and albino SD rat strains had implicated ocular pigmentation in susceptibility to hypoxia in the oxygen-induced retinopathy model.[33] A biphasic oxygen-exposure protocol similar to the one described in this study, comprising an initial hyperoxic exposure followed by a period of relative hypoxia in room air, was used. Retinal vascular abnormalities were more marked in the BN strain after the period of relative hypoxia. This was associated with a higher ratio of expression of VEGF to the antiangiogenic factor pigment epithelium derived factor (PEDF), in the BN compared with the SD strain. Accordingly, the BN strain was deemed to be more susceptible to retinal hypoxia. However, allowance was not made for the relative susceptibilities of each strain to the initial hyperoxic exposure. It was noted that BN retinas were less well vascularized than those of the SD strain immediately after hyperoxic exposure. Thus, the stimulus for angiogenic factor expression was not equal for the different rat strains at the commencement of room air exposure. It follows that the observed differences in angiogenic factor expression and retinal vascularization may have been due to a greater susceptibility to hyperoxia of the BN rat, rather than to differences in the response to hypoxia.

The two rat strains most susceptible to hyperoxia in the present study, the HW and DA, were also those with pigmented eyes. PEDF was first purified from extracts of cultured retinal pigment epithelial (RPE) cells.[55] Oxygen excess has been associated with an increase in retinal PEDF expression in vivo and in RPE cell culture,[56,57] but the mechanisms of this effect are yet to be determined. It may be that pigmented eyes express PEDF to a greater extent under hyperoxia than do nonpigmented eyes. This difference would lead to an increase in PEDF-mediated inhibition of retinal angiogenesis during the hyperoxic exposure, rendering the retinas of pigmented eyes more ischemic on room air exposure. In the study of Gao et al.,[33] retinal PEDF expression was increased 3.8-fold over control samples from BN rats at the conclusion of hyperoxic exposure. No significant increase in PEDF levels was found in SD rats at the same time point, supporting this hypothesis. However, the greater susceptibility of the SD strain compared with the other albino strains in the present study, suggests that factors other than ocular pigmentation must also be important.

Studies of human ROP do not support the conclusion that ocular pigmentation is positively associated with the severity of disease. In fact, multivariate analysis of data collected from 4099 premature neonates in the natural history cohort of the Cryotherapy for Retinopathy of Prematurity (CRYO-ROP) study suggests the converse.[58] White neonates were at significantly greater risk of severe retinopathy than black neonates. This finding reinforces the fact that the rodent model of oxygen-induced retinopathy is an approximation of a complex and multifactorial human disease and that care must be taken in the extrapolation of findings from the animal model. The basis for the association between ocular pigmentation and the risk of retinopathy in humans and rodents remains uncertain.

Strain-dependent differences in the susceptibility to hyperoxia may in part account for the abandonment of the rat model of oxygen-induced retinopathy for >30 years. In the 1950s and early 1960s Ashton and Blach.[59] were unable to demonstrate significant retinopathy in WF rat pups in studies of oxygen-induced retinopathy. The present study identified the WF strain as relatively resistant to hyperoxic exposure. It was not until the 1990s that the rat model became widely accepted as a valid model of proliferative retinopathy, due largely to the studies of Reynaud and Penn,[18,20,37,38] who exposed the more susceptible SD strain to cyclic hyperoxia.

Strain-related heterogeneity of ocular angiogenesis in rodents is not limited to susceptibility to hyperoxia. Rohan et al.[60] have identified strain-dependent variation in the response to angiogenic factors. In a mouse model of corneal neovascularization, corneal stromal implantation of basic fibroblast growth factor (bFGF)–impregnated micropellets was associated with angiogenesis that differed by up to 10-fold among strains. Similar heterogeneity was seen in the response to VEGF. Chan et al.[61] have demonstrated that the extent of the resting limbal vasculature differs considerably among mouse strains and is predictive of the response to bFGF in the corneal neovascularization model.

Identification of the etiology of the strain-related differences described in this study will enhance understanding of the rodent model of oxygen-induced retinopathy. This determination is of importance, given the increasing use of the model for studies of the pathogenesis of the human proliferative retinopathies and the trial of potential therapeutic interventions.[62] Further work may lead to the identification of genetic risk factors for human ROP, allowing the stratification and treatment of at-risk neonates.

Acknowledgments

The authors thank Anne-Louise Smith for engineering expertise and Ray Yates for animal husbandry.

References

1. Early treatment diabetic retinopathy study research group. Early photocoagulation for diabetic retinopathy. ETDRS report number 9. *Ophthalmology*. 1991;98:766–785.
2. Zimmer-Galler IE, Bressler NM, Bressler SB. Treatment of choroidal neovascularization: updated information from recent macular photocoagulation study group reports. *Int Ophthalmol Clin*. 1995;35: 37–57.
3. Quinn GE, Dobson V, Barr CC, et al. Visual acuity in infants after vitrectomy for severe retinopathy of prematurity. *Ophthalmology*. 1991;98:5–13.
4. Pierce EA, Foley ED, Smith LE. Regulation of vascular endothelial growth factor by oxygen in a model of retinopathy of prematurity. *Arch Ophthalmol*. 1996;114:1219–1228.
5. Aiello LP. Vascular endothelial growth factor. 20th-century mechanisms, 21st-century therapies. *Invest Ophthalmol Vis Sci*. 1997; 38:1647–1652.
6. Michaelson IC. *Retinal Circulation in Man and Animals.* Springfield, IL: CC Thomas; 1954.
7. Ashton N, Ward B, Serpell G. Effect of oxygen on developing retinal vessels with particular reference to the problem of retrolental fibroplasia. *Br J Ophthalmol*. 1954;38:397–432.
8. Chan-Ling T, Stone J. Retinopathy of prematurity: its origins in the architecture of the retina. *Prog Ret Res*. 1993;12:155–178.
9. Stone J, Itin A, Alon T, et al. Development of retinal vasculature is mediated by hypoxia-induced vascular endothelial growth factor (VEGF) expression by neuroglia. *J Neurosci*. 1995;15:4738–4747.
10. Pierce EA, Avery RL, Foley ED, Aiello LP, Smith LE. Vascular endothelial growth factor/vascular permeability factor expression in a mouse model of retinal neovascularization. *Proc Nat Acad Sci USA*. 1995;92:905–909.
11. Dorey CK, Aouididi S, Reynaud X, Dvorak HF, Brown LF. Correlation of vascular permeability factor/vascular endothelial growth factor with extraretinal neovascularization in the rat. *Arch Ophthalmol*. 1996;114:1210–1217.
12. Alon T, Hemo I, Itin A, Pe'er J, Stone J, Keshet E. Vascular endothelial growth factor acts as a survival factor for newly formed retinal vessels and has implications for retinopathy of prematurity. *Nat Med*. 1995;1:1024–1028.
13. Wang GL, Semenza GL. Purification and characterization of hypoxia-inducible factor 1. *J Biol Chem*. 1995;270:1230–1237.
14. Semenza GL. HIF-1: mediator of physiological and pathophysiological responses to hypoxia. *J Appl Physiol*. 2000;88:1474–1480.
15. Semenza GL. Regulation of hypoxia-induced angiogenesis: a chaperone escorts VEGF to the dance. *J Clin Invest*. 2001;108:39–40.
16. Linsenmeier RA, Yancey CM. Effects of hyperoxia on the oxygen distribution in the intact cat retina. *Invest Ophthalmol Vis Sci*. 1989;30:612–618.
17. Alder VA, Ben-Nun J, Cringle SJ. PO_2 profiles and oxygen consumption in cat retina with an occluded retinal circulation. *Invest Ophthalmol Vis Sci*. 1990;31:1029–1034.
18. Reynaud X, Dorey CK. Extraretinal neovascularization induced by hypoxic episodes in the neonatal rat. *Invest Ophthalmol Vis Sci*. 1994;35:3169–3177.
19. Madan A, Penn JS. Animal models of oxygen-induced retinopathy. *Front Biosci*. 2003;8:1030–1043.
20. Penn JS, Tolman BL, Henry MM. Oxygen-induced retinopathy in the rat: relationship of retinal nonperfusion to subsequent neovascularization. *Invest Ophthalmol Vis Sci*. 1994;35:3429–3435.
21. Holmes JM, Zhang S, Leske DA, Lanier WL. Metabolic acidosis-induced retinopathy in the neonatal rat. *Invest Ophthalmol Vis Sci*. 1999;40:804–809.
22. Holmes JM, Duffner LA, Kappil JC. The effect of raised inspired carbon dioxide on developing rat retinal vasculature exposed to elevated oxygen. *Curr Eye Res*. 1994;13:779–782.
23. Holmes JM, Leske DA, Zhang S. The effect of raised inspired carbon dioxide on normal retinal vascular development in the neonatal rat. *Curr Eye Res*. 1997;16:78–81.
24. Holmes JM, Zhang S, Leske DA, Lanier WL. Carbon dioxide-induced retinopathy in the neonatal rat. *Curr Eye Res*. 1998;17:608–616.
25. Holmes JM, Duffner LA. The effect of postnatal growth retardation on abnormal neovascularization in the oxygen exposed neonatal rat. *Curr Eye Res*. 1996;15:403–409.
26. Zhang S, Leske DA, Lanier WL, Holmes JM. Postnatal growth retardation exacerbates acidosis-induced retinopathy in the neonatal rat. *Curr Eye Res*. 2001;22:133–139.
27. Smith LE, Shen W, Perruzzi C, et al. Regulation of vascular endothelial growth factor-dependent retinal neovascularization by insulin-like growth factor-1 receptor. *Nat Med*. 1999;5:1390–1395.
28. Hellstrom A, Perruzzi C, Ju M, et al. Low IGF-1 suppresses VEGF-survival signaling in retinal endothelial cells: direct correlation with clinical retinopathy of prematurity. *Proc Nat Acad Sci USA*. 2001;98:5804–5808.
29. Brooks SE, Gu X, Samuel S, et al. Reduced severity of oxygen-induced retinopathy in eNOS-deficient mice. *Invest Ophthalmol Vis Sci*. 2001;42:222–228.
30. Lutty GA, Merges C, McLeod DS. 5′ Nucleotidase and adenosine during retinal vasculogenesis and oxygen-induced retinopathy. *Invest Ophthalmol Vis Sci*. 2000;41:218–229.
31. Wilkinson-Berka JL, Alousis NS, Kelly DJ, Gilbert RE. COX-2 inhibition and retinal angiogenesis in a mouse model of retinopathy of prematurity. *Invest Ophthalmol Vis Sci*. 2003;44:974–979.
32. Nunes I, Higgins RD, Zanetta L, Shamamian P, Goff SP. c-abl is required for the development of hyperoxia-induced retinopathy. *J Exp Med*. 2001;193:1383–1391.
33. Gao G, Li Y, Fant J, Crosson CE, Becerra SP, Ma JX. Difference in ischemic regulation of vascular endothelial growth factor and pigment epithelium-derived factor in Brown Norway and Sprague Dawley rats contributing to different susceptibilities to retinal neovascularization. *Diabetes*. 2002;51:1218–1225.
34. Safa R, Osborne NN. Retinas from albino rats are more susceptible to ischaemic damage than age-matched pigmented animals. *Brain Res*. 2000;862:36–42.
35. Engelmann R, Dieterich DC, Bien A, Kreutz MR. A different retinal glia response to optic nerve injury/lipopolysaccharide administration in hooded and albino rats. *Brain Res*. 2001;889:251–255.
36. Ventresca MR, Gonder JR, Tanswell AK. Oxygen-induced proliferative retinopathy in the newborn rat. *Can J Ophthalmol*. 1990;25: 186–189.
37. Penn JS, Tolman BL, Lowery LA. Variable oxygen exposure causes preretinal neovascularization in the newborn rat. *Invest Ophthalmol Vis Sci*. 1993;34:576–585.
38. Penn JS, Henry MM, Wall PT, Tolman BL. The range of PaO2 variation determines the severity of oxygen-induced retinopathy in newborn rats. *Invest Ophthalmol Vis Sci*. 1995;36:2063–2070.
39. Chan-Ling T. Glial, vascular, and neuronal cytogenesis in whole-mounted cat retina. *Microsc Res Tech*. 1997;36:1–16.
40. Hayes CE, Goldstein IJ. An α-D-galactosyl-binding lectin from *Bandeiraea simplicifolia* seeds: isolation by affinity chromatography and characterization. *J Biol Chem*. 1974;249:1904–1914.
41. Cunningham S, McColm JR, Wade J, Sedowofia K, McIntosh N, Fleck B. A novel model of retinopathy of prematurity simulating preterm oxygen variability in the rat. *Invest Ophthalmol Vis Sci*. 2000;41:4275–4280.
42. Zhang S, Leske DA, Holmes JM. Neovascularization grading methods in a rat model of retinopathy of prematurity. *Invest Ophthalmol Vis Sci*. 2000;41:887–891.
43. Sokal RR, Rohlf FJ. *Biometry: The Principles and Practice of Statistics in Biological Research.* 3rd ed. New York: Freeman; 1995.
44. The Committee for the Classification of Retinopathy of Prematurity. An international classification of retinopathy of prematurity. *Arch Ophthalmol*. 1984;102:1130–1134.
45. Chan-Ling T, Stone J. Degeneration of astrocytes in feline retinopathy of prematurity causes failure of the blood-retinal barrier. *Invest Ophthalmol Vis Sci*. 1992;33:2148–2159.
46. Stone J, Chan-Ling T, Pe'er J, Itin A, Gnessin H, Keshet E. Roles of vascular endothelial growth factor and astrocyte degeneration in

the genesis of retinopathy of prematurity. *Invest Ophthalmol Vis Sci*. 1996;37:290–299.

47. Dorrell MI, Aguilar E, Friedlander M. Retinal vascular development is mediated by endothelial filopodia, a preexisting astrocytic template and specific R-cadherin adhesion. *Invest Ophthalmol Vis Sci*. 2002;43:3500–3510.
48. Ashton N, Ward B, Serpell G. Role of oxygen in the genesis of retrolental fibroplasia. *Br J Ophthalmol*. 1953;37:513–520.
49. McLeod DS, Brownstein R, Lutty GA. Vaso-obliteration in the canine model of oxygen-induced retinopathy. *Invest Ophthalmol Vis Sci*. 1996;37:300–311.
50. Asahara T, Murohara T, Sullivan A, et al. Isolation of putative progenitor endothelial cells for angiogenesis. *Science*. 1997;275:964–967.
51. Grant MB, May WS, Caballero S, et al. Adult hematopoietic stem cells provide functional hemangioblast activity during retinal neovascularization. *Nat Med*. 2002;8:607–612.
52. Pandey J, Bannout A, Wendell DL. The Edpm5 locus prevents the "angiogenic switch" in an estrogen-induced rat pituitary tumor. *Carcinogenesis*. 2004;25:1829–1838.
53. Wang H, Olszewski B, Rosebury W, Wang D, Robertson A, Keiser JA. Impaired angiogenesis in SHR is associated with decreased KDR and MT1-MMP expression. *Biochem Biophys Res Commun*. 2004;315:363–368.
54. Kitzmann A, Leske D, Chen Y, Kendall A, Lanier W, Holmes J. Incidence and severity of neovascularization in oxygen- and metabolic acidosis-induced retinopathy depend on rat source. *Curr Eye Res*. 2002;25:215–220.
55. Tombran-Tink J, Johnson LV. Neuronal differentiation of retinoblastoma cells induced by medium conditioned by human RPE cells. *Invest Ophthalmol Vis Sci*. 1989;30:1700–1707.
56. Gao G, Li Y, Zhang D, Gee S, Crosson C, Ma J. Unbalanced expression of VEGF and PEDF in ischemia-induced retinal neovascularization. *FEBS Lett*. 2001;489:270–276.
57. Dawson DW, Volpert OV, Gillis P, et al. Pigment epithelium-derived factor: a potent inhibitor of angiogenesis. *Science*. 1999;285:245–248.
58. Saunders RA, Donahue ML, Christmann LM, et al. Racial variation in retinopathy of prematurity. The Cryotherapy for Retinopathy of Prematurity Cooperative Group. *Arch Ophthalmol*. 1997;115:604–608.
59. Ashton N, Blach R. Studies on developing retinal vessels VIII. Effect of oxygen on the retinal vessels of the ratling. *Br J Ophthalmol*. 1961;45:321–340.
60. Rohan RM, Fernandez A, Udagawa T, Yuan J, D'Amato RJ. Genetic heterogeneity of angiogenesis in mice. *FASEB J*. 2000;14:871–876.
61. Chan CK, Pham LN, Chinn C, et al. Mouse strain-dependent heterogeneity of resting limbal vasculature. *Invest Ophthalmol Vis Sci*. 2004;45:441–447.
62. Mechoulam H, Pierce EA. Retinopathy of prematurity: molecular pathology and therapeutic strategies. *Am J Pharmacogenomics*. 2003;3:261–277.